Effects of Macromolecular Crowding on Biochemical Reaction Equilibria: A Molecular Thermodynamic Perspective

Zhongqiao Hu,* Jianwen Jiang,*† and Raj Rajagopalan*†

*Department of Chemical and Biomolecular Engineering and †The Singapore-MIT Alliance, National University of Singapore, Singapore 117576

ABSTRACT A molecular thermodynamic model is developed to investigate the effects of macromolecular crowding on biochemical reactions. Three types of reactions, representing protein folding/conformational isomerization, coagulation/coalescence, and polymerization/association, are considered. The reactants, products, and crowders are modeled as coarse-grained spherical particles or as polymer chains, interacting through hard-sphere interactions with or without nonbonded square-well interactions, and the effects of crowder size and chain length as well as product size are examined. The results predicted by this model are consistent with experimentally observed crowding effects based on preferential binding or preferential exclusion of the crowders. Although simple hard-core excluded-volume arguments do in general predict the qualitative aspects of the crowding effects, the results show that other intermolecular interactions can substantially alter the extent of enhancement or reduction of the equilibrium and can even change the direction of the shift. An advantage of the approach presented here is that competing reactions can be incorporated within the model.

INTRODUCTION: CROWDING IN BIOLOGICAL SYSTEMS

Because biological cells consist of a large number of macromolecular crowders such as polymers, protein tubulins, and actin fibers, which could occupy as much as 40% of the total volume (1), and this physical crowding can significantly alter the biophysical and chemical properties of live cells and can subsequently lead to substantial effects on biomolecular functions and cellular evolution processes (2). The effects of crowding are often attributed to the increase in the volume excluded for the biochemically functional species (''reactants'' and ''products''). In other words, a reactant or a product can occupy only a part of the total volume as the available volume decreases because of the presence of the crowders. Crowding plays a pivotal role in a number of key chemical and biochemical reactions and phenomena; examples include protein folding and stability (3,4), isomerization (5), self- or heteroassociation (4,6,7), enzyme-catalyzed reactions (8,9), and sedimentation equilibria (10). It has also been demonstrated that in a highly crowded medium such as a cell, the reactivity of one species could be enhanced by several orders of magnitude and could vary with the relative sizes of the reactant, product, and crowder as well as with the crowder concentration.

At the microscopic level, the effects of crowding are largely attributed to the steric repulsion among the different types of species. A number of theoretical studies have been reported in the literature, with qualitative or semiquantitative simplifications for intermolecular interactions as well as for the shapes and conformations of molecules, to describe the consequences of steric repulsion on reactions. For example, using the hard-particle approximation, Minton (11) employed the scaled-particle theory and lattice theory to examine the effects of crowding on the thermodynamic activity of globular macromolecules and macromolecular complexes. Minton and Edelhoch (12) used this model to interpret the light-scattering data on bovine serum albumin (BSA) at different concentrations and pHs. The effective hard-particle model was further used by Minton (13) to calculate the osmotic pressure of BSA as a function of protein concentration and pH in a buffer solution with 0.1 mol/L NaCl. Recently, Minton (14) proposed a thermodynamic model to study the inert macromolecular crowding effect on the stability of a globular protein. Berg (15) developed a hard-particle model by including the primary solvent as a separate component in a hard-sphere (HS) mixture and examined the influence of macromolecular crowding on solubility and dimerization constant for spherical and dumbbell-shaped molecules. Zhou and Hall (16) developed a statistical thermodynamic theory to investigate the effect of solute-excluded volume on the stability of globular proteins at infinite dilution. Alternatively, a density functional theory has been adapted by Kinjo and Takada (17,18) to explore the excluded-volume effect in inhomogeneous solutions by assuming a hard-core square-well (SW) potential between denatured protein molecules.

Recently, molecular simulations have also been reported to explore crowding effects on protein folding and aggregation (18–22). For instance, Elcock (22) employed Brownian dynamics to calculate the free energy of transfer for a rigid globular rhodanese molecule from the hollow interior of a GroEL chaperone protein into bulk solvent as a function

Submitted January 19, 2007, and accepted for publication April 12, 2007.

Address reprint requests to Jianwen Jiang, Dept. of Chemical and Biomolecular Engineering, National University of Singapore, 4 Engineering Dr. 4, Singapore 117576. E-mail: chejj@nus.edu.sg.

Editor: Ruth Nussinov.

0006-3495/07/09/1464/10 $2.00

doi: 10.1529/biophysj.107.104646

of the volume fraction of solvent occupied by a rigid inert crowding reagent. The advantage of molecular simulations is that they can be readily employed to treat (relatively) idealized systems using models based on simple molecular interactions (e.g., HS potentials and simplified repulsive and attractive interactions) and consequently can provide insights from a microscopic perspective, although the models themselves may not be fully realistic because of their neglect of any significant nonadditive and/or long-range interactions that may be present. In principle, more elaborate simulations with detailed atomic-level descriptions of the crowders and reacting species are formally within reach, but the computational efforts needed are invariably beyond reach in practice. Nevertheless, resorting to simulations is not convenient in practice; therefore, molecular thermodynamic theories based on a sound statistical mechanical representation for thermodynamic contributions of the various species are an attractive option to explore.

The objective of this work is to develop a simple molecular thermodynamic formalism based on statistical thermodynamic principles to investigate the effects of macromolecular crowding. To this end, we consider inert crowders and examine their effects on the equilibria of chemical reactions, using the polymeric SW chain model within the molecular thermodynamic formalism. In addition to the HS excluded-volume effect, a short-range attractive interaction is also considered and is shown to play a significant quantitative role in influencing the reaction equilibria, although the qualitative aspects of the influence of the crowders are determined by the hard-core excluded-volume interactions. In the next section, we begin with a description of the proposed molecular thermodynamic model. We then employ this model to study the effects of crowding on three types of chemical or biochemical reactions, namely, protein folding, coagulation (or coalescence), and polymerization (or association). The predicted results are compared with those from the HS chain model. General conclusions are then summarized.

MOLECULAR THERMODYNAMIC FORMULATION OF REACTIONS UNDER CROWDED CONDITIONS

In this section we develop the basic molecular thermodynamic formulation for determining the degree of reaction α for a reaction in a crowded environment. The approach involves calculating α from its relation to the reaction equilibrium constant as a function of the activities of the reactant and product, with the activities determined using suitable statistical thermodynamic theories based on appropriate models of molecular interactions.

Degree of reaction and equilibrium constant

For the present purpose, we consider a general chemical reaction as shown schematically in Fig. 1

$$nR \rightleftharpoons P, \tag{1}$$

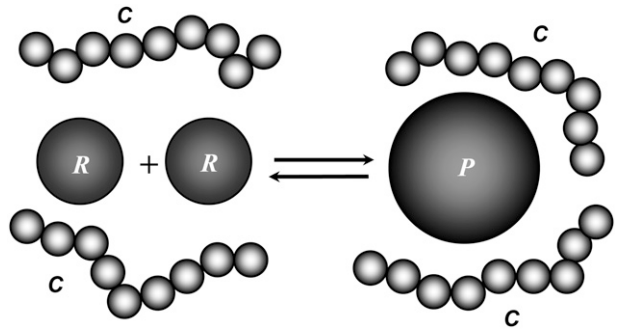

FIGURE 1 Schematic illustration of a chemical reaction $nR \rightleftharpoons P$ in the presence of crowder C. Although the reactant and the product are shown as spherical whereas the crowder is represented as a chainlike molecule, the theoretical formalism presented in the article allows each of them to be either spherical or chainlike.

where R is the reactant and P is the product, presumed to be distributed in a sea of crowder, denoted as C in Fig. 1. The reactant and the product, as well as the crowder, may be simple spherical molecules or chainlike molecules. Although formally simple, the reaction shown in Eq. 1 is sufficient to study a variety of situations such as folding transition of a chain molecule and coagulation or polymerization of particles, as we discuss subsequently. The initial concentrations of R and P are denoted by c_R^0 and c_P^0, respectively. For simplicity, we assume $c_P^0 = 0$. The concentration of the crowder is c_C, which is assumed to remain constant during the reaction. If the degree of reaction is α, the concentrations of R and P at equilibrium are $c_R^0(1-\alpha)$ and $c_R^0\alpha/n$, respectively. The thermodynamic equilibrium constant $K^{\ominus}$ is then

$$K^{\ominus} = \frac{\left(c_R^0\alpha/n\right)\gamma_P}{\left[c_R^0(1-\alpha)\gamma_R\right]^n} = \frac{\alpha\gamma_P}{n\left(c_R^0\right)^{n-1}\left[(1-\alpha)\gamma_R\right]^n}, \tag{2}$$

where the γs are the activity coefficients. The equilibrium constant $K^{\ominus}$ is constant at a given temperature. We define the stoichiometric equilibrium constant K as

$$K = \frac{\left(c_R^0\alpha/n\right)}{\left[c_R^0(1-\alpha)\right]^n} = K^{\ominus}\frac{\gamma_R^n}{\gamma_P}. \tag{3}$$

Both K and α are related to the activity coefficients, which depend on the type, size, and concentration of the crowder, as they affect the reactant and product concentrations as we shall see subsequently. At infinite dilution, the activity coefficients approach unity, and therefore K approaches $K^{\ominus}$.

Our objective is to determine the degree of reaction α using Eq. 3 for a given type of reaction with a known initial concentration of the reactant and a given equilibrium constant for any arbitrary crowder concentration, so that the effect of the crowder on the enhancement or reduction of the extent of reaction may be examined. To use Eq. 3, however, one needs the values of the activity coefficients of the reactant and the product as functions of the respective concentrations. To obtain the activity coefficients, we use

standard statistical/molecular thermodynamic formalisms and treat the mixture of reactant, product, and crowder as a multicomponent system.

Molecular thermodynamic model of activity coefficients

Without loss of generality, we represent the reactant, product, and crowder as chain molecules with number density ρ_i, chain length m_i, and segment diameter σ_i (i = R, P, C). When $m_i = 1$, a spherical molecule is recovered. In addition to the HS interactions between segments (monomers) implied by the above prescription, the short-range interactions between the nonbonded segments is modeled by the SW potential:

$$u_{ij}(r) = \begin{cases} \infty & r < \sigma_{ij} \\ -\varepsilon_{ij} & \sigma_{ij} < r < \lambda_{ij}\sigma_{ij} \\ 0 & r > \lambda_{ij}\sigma_{ij} \end{cases}, \quad (4)$$

where $\sigma_{ij} = (\sigma_i + \sigma_j)/2$ is the additive HS diameter, $\varepsilon_{ij} = \sqrt{\varepsilon_i \varepsilon_j}$ is the cross well depth, and $\lambda_{ij} = (\lambda_i\sigma_i + \lambda_j\sigma_j)/(\sigma_i + \sigma_j)$ is the cross well width. This model reduces to a simple hard-sphere chain (HSC) model by setting $\varepsilon_i = \varepsilon_j = 0$ or $\lambda_i = \lambda_j = 1$.

We consider three contributions to the excess Helmholtz energy A^{ex} of the multicomponent mixture, namely, contribution from the size of the molecules or by the individual segments in the case of chainlike molecules (represented by HS interactions), contribution from nonbonded interactions between segments (represented by attractive SW interactions), and contributions from chain formation; i.e.,

$$A^{ex} = A^{hs} + A^{sw} + A^{chain}. \quad (5)$$

The HS contribution can be written as (23)

$$\frac{\beta A^{hs}}{V} = \left(\frac{\zeta_2^3}{\zeta_3^2} - \zeta_0\right)\ln\Delta + \frac{(\pi\zeta_1\zeta_2/2) - (\zeta_2^3/\zeta_3^2)}{\Delta} + \frac{\zeta_2^3/\zeta_3^2}{\Delta^2}, \quad (6)$$

where $\zeta_l = \sum_i m_i\rho_i\sigma_i^l$ and $\Delta = 1 - \pi\zeta_3/6$.

The SW contribution can be evaluated using the second-order Baker-Henderson perturbation theory (24):

$$\frac{\beta A^{sw}}{V} = \frac{1}{\zeta_0}\sum_i\sum_j m_i m_j \rho_i \rho_j \left(\beta a_1^{ij} + \beta^2 a_2^{ij}\right), \quad (7)$$

where the mean attractive energy a_1^{ij} is given by a compact expression from the mean-value theorem (25):

$$\beta a_1^{ij} = -\frac{2}{3}\pi\zeta_0\sigma_{ij}^3(\beta\varepsilon_{ij})\left(\lambda_{ij}^3 - 1\right)g_{ij}^{hs}\left(\sigma_{ij}, \zeta_3^{eff}\right). \quad (8)$$

In Eq. 8, $g_{ij}^{hs}(\sigma_{ij})$ is the pair correlation function of hard spheres at contact and is evaluated at an effective packing fraction ζ_3^{eff}:

$$g_{ij}^{hs}(\sigma_{ij}) = \frac{1}{\Delta} + \frac{\pi\sigma_i\sigma_j\zeta_2}{4\Delta^2\sigma_{ij}} + \frac{\pi^2\sigma_i^2\sigma_j^2\zeta_2^2}{72\Delta^3\sigma_{ij}^2}. \quad (9)$$

The second perturbation term a_2^{ij} in Eq. 7 describing the fluctuations of attractive energy is given by

$$\beta^2 a_2^{ij} = \frac{\zeta_0^2\Delta^4(\beta\varepsilon_{ij})}{2\left(\zeta_0\Delta^2 + \pi\zeta_1\zeta_2\Delta + \pi^2\zeta_2^3/4\right)}\frac{\partial\left(\beta a_1^{ij}\right)}{\partial\zeta_0}. \quad (10)$$

The contribution from chain connectivity can be obtained from thermodynamic perturbation theory as used in the development of the statistical-associating-fluid theory (SAFT) (26) and of the equation of state for chain fluids (27)

$$\frac{\beta A^{chain}}{V} = \sum_i \rho_i(1 - m_i)\ln y_{ii}^{sw}(\sigma_i), \quad (11)$$

where the cavity correlation function $y_{ii}^{sw}(\sigma_i)$ at contact is defined by

$$y_{ii}^{sw}(\sigma_i) = g_{ii}^{sw}(\sigma_i)\exp(-\beta\varepsilon_i) \quad (12)$$

with

$$g_{ii}^{sw}(\sigma_i) = g_{ii}^{hs}(\sigma_i) + \frac{1}{2\pi\zeta_0\sigma_i^3}\left(3\zeta_0\frac{\partial\left(\beta a_1^{ii}\right)}{\partial\zeta_0} - \lambda_i\frac{\partial\left(\beta a_1^{ii}\right)}{\partial\lambda_i}\right). \quad (13)$$

Finally, the activity coefficient can be calculated from

$$\ln\gamma_i = \left(\frac{\partial(\beta A^{ex}/V)}{\partial\rho_i}\right)_{T,V,\rho_{j[i]}}. \quad (14)$$

Equations 5–14 allow us to determine the activity coefficients of the various species (particularly those of the reactant and product) at any concentration (or, equivalently, at any degree of reaction α). Therefore, Eq. 3 can now be solved (iteratively) for α for any given equilibrium constant $K^{\ominus}$, initial concentration of the reactant c_R^0, and stoichiometric coefficient n, as a function of any arbitrary crowder concentration. In what follows, we use this procedure to examine the effects of crowding for a number of reactions.

RESULTS AND DISCUSSION

We examine here three reactions of practical interest, namely, 1), folding of a denatured protein, 2), coagulation of a protein, and 3), polymerization of a monomer. The first corresponds to conformational isomerization reaction in which a polymer/biopolymer with an expanded, chainlike conformation changes to a collapsed, compact spherical conformation (as modeled here). The second corresponds to coalescence of small spherical reactants to a large spherical product or to globular protein forming a globular ''amorphous'' molten globular product. The last represents the type of macromolecular self-association reaction described by Minton (4).

Our primary objective here is to capture the qualitative and relatively quantitative aspects of the effects of the crowders on the degree of reaction and examine the predictions of the molecular thermodynamic approach. Therefore, the molecules or the segments (in chainlike molecules) are modeled simply as spherical. We fix the thermodynamic equilibrium constant $K^{\ominus}$ at unity and take the SW width, λ_i, and the SW

depth, (ε_i/k_B), as, respectively, 1.5 and 30 K (or, equivalently, ε_i to be $\sim 0.4 \times 10^{-21}$ J or 0.25 kJ/mol at a room temperature of 25°C) for all species (i.e., reactant, product, as well as crowder). In each case, an initial concentration for the reactant is assumed (as indicated in the figure captions), and the degree of reaction is calculated for various crowder concentrations.

Protein folding (or isomerization)

We begin with an examination of the folding/unfolding of ubiquitin. The process is simplified as a dynamic equilibrium between the denatured and native ubiquitin,

$$R_{76} \rightleftharpoons P, \tag{15}$$

where the denatured ubiquitin is modeled as an elongated flexible chain composed of 76 spherical segments (denoted by R_{76}), with each segment representing one amino acid residue with a size of 0.38 nm, as suggested elsewhere (16,28). The native ubiquitin is modeled as a macrosphere with diameter of 2.4 nm, based on the available experimental x-ray scattering data for the radius of gyration (29); subsequently deviations from this value will be examined to assess the sensitivity of the results. Despite the variety of structural manifolds involved, numerous observations demonstrate that the above two-state model captures the underlying physics in protein folding/unfolding reasonably well (30).

The effect of crowder on the activity coefficients of reactant R_{76} and product P is examined first for the folding of ubiquitin at an initial concentration of the denatured protein $c_R^0 = 0.013\,\text{mol/L}$ (i.e., the segment density is $0.013 \times 76 = 1$ mol/L). Both $\gamma_{R_{76}}$ and γ_P (not shown) are found to increase monotonically with crowder concentration. The magnitude of increase is very significant: both $\gamma_{R_{76}}$ and γ_P could reach astronomical numbers at high crowder concentrations. The activity coefficients are predominantly determined by the HS interactions and slightly decrease when the short-ranged attractive SW interactions are incorporated. Fig. 2 shows the activity coefficient of reactant over that of product $(\gamma_{R_{76}}/\gamma_P)$ as a function of crowder concentration at three different sizes of the crowder. With increasing crowder concentration, $\gamma_{R_{76}}/\gamma_P$ drops consistently for a small crowder with $\sigma_C = 0.3\,\text{nm}$; rises negligibly and then drops for $\sigma_C = 0.4\,\text{nm}$; rises to a maximum and then drops rapidly for $\sigma_C = 0.5\,\text{nm}$. The crowding effect is substantial on the activity coefficients of both reactant and product, which subsequently leads to a drastic change in the degree of reaction.

Fig. 3 shows the degree of reaction α for the folding of ubiquitin for pure HS interactions (with the protein modeled as an HSC, i.e., a string of hard spheres) as well as for the situation with additional SW nonbonded interactions. At the outset, we note from the results of the HSC model that the hard-core excluded volume alone (i.e., just the hard-core interactions) largely determines the qualitative behavior of

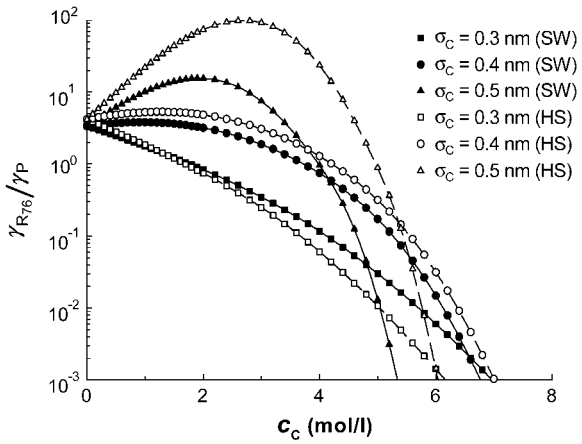

FIGURE 2 Activity coefficient of reactant over that of product for folding $R_{76} \rightleftharpoons P$ as a function of the molar concentration of crowder C. Solid lines correspond to situations in which nonbonded SW interactions are included, whereas the dashed lines correspond to only the HS interactions. It has been assumed that $c_R^0 = 0.013\,\text{mol/l}$, $m_R = 76$, $\sigma_R = 0.38\,\text{nm}$, $m_P = 1$, $\sigma_P = 2.40\,\text{nm}$, and $m_C = 1$.

the crowding effect. We have used our model to examine the folding of bovine pancreatic trypsin inhibitor (BPTI) as studied by Zhou and Hall (16). Our model reproduces their results at low crowder concentrations (that is, for crowder concentrations corresponding to well below the Kirkwood-Alder freezing transition for spherical crowders), as should be expected. The results of Zhou and Hall, however, predict unrealistically high enhancement in the reaction equilibrium, by ~8 orders of magnitude, for spherical crowders at a volume fraction of ~0.6, beyond the freezing (i.e., Kirkwood-Alder) limit for the structure of the crowders. We suspect that the equations used for the pressures and chemical potentials break down in this limit in the calculations presented by Zhou and Hall. Our results reveal, however, that other interactions (e.g., attractive interactions among the various species) can have a strong influence on the quantitative aspects. For example, it is evident from the figure that the short-ranged SW attractions change the magnitude of the degree of reaction, with the results leading to generally smaller α, although the overall qualitative behavior remains unaffected. In other words, entropic effects dominate the qualitative effects of crowding quite well, but enthalpic considerations are necessary to obtain quantitative guidance.

To explore the role of the various parameters on crowding, we begin with an examination of the effect of crowder size. Fig. 3 *a* corresponds to single, spherical crowders ($m_C = 1$) of size σ_C, with denatured and native ubiquitin of fixed sizes. For small $\sigma_C = 0.3\,\text{nm}$, α decreases monotonically with increasing c_C because, as can be shown through simple geometric arguments, the unfolded conformations of the protein exclude less volume for the relatively small crowder molecules. Conformations of the protein that allow more available volume for the crowders are naturally entropically more stable. This situation, however, changes for larger crowders,

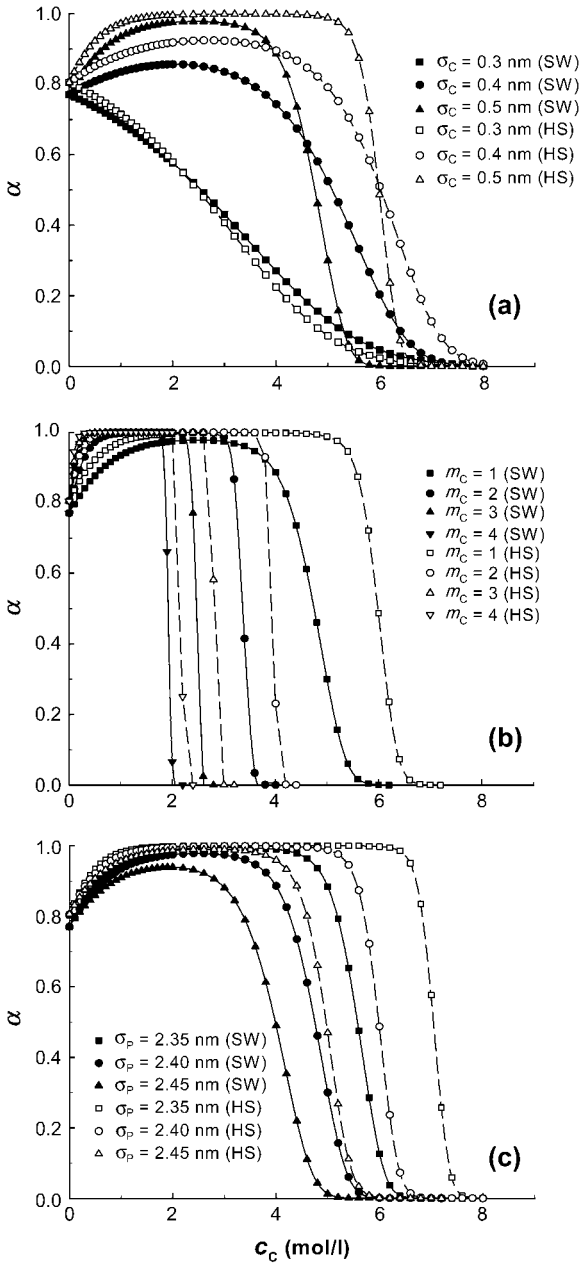

FIGURE 3 Degree of reaction α for folding $R_{76} \rightleftharpoons P$ as a function of the molar concentration of crowder C. Solid lines correspond to situations in which nonbonded SW interactions are included, whereas the dashed lines correspond to only the HS interactions. For all the three cases shown below, it has been assumed that $c_R^0 = 0.013\,\text{mol/l}$, $m_R = 76$, $\sigma_R = 0.38\,\text{nm}$, $m_P = 1$. (*a*) The effect of the size of crowder: $\sigma_P = 2.40\,\text{nm}$, $m_C = 1$. (*b*) The effect of the chain length of crowder: $\sigma_P = 2.40\,\text{nm}$, $\sigma_C = 0.5\,\text{nm}$. (*c*) The effect of the size of product: $\sigma_C = 0.5\,\text{nm}$, $m_C = 1$.

e.g., at $\sigma_C = 0.4$ or 0.5 nm or larger, and, therefore, whether the crowder promotes or impedes stability of the unfolded form depends further on the crowder concentration c_C. At low c_C the spherical native ubiquitin excludes less volume than the chainlike denatured ubiquitin does, and this preferential exclusion of the crowder by the unfolded chains drives folding. However, beyond a limit, at high c_Cs, the unfolded conformations prevail over the folded form and allow more volume for the crowder, and, as a consequence, the degree of reaction decreases. For even larger crowders (not shown here), α is found to remain closer to unity over a wide range of c_C; i.e., the denatured ubiquitin completely folds into the native state before the equilibrium shifts sharply toward the unfolded form at very high concentrations. In general, the results predict that there is an optimum concentration range for the crowder over which the folding transition is enhanced.

The qualitative aspects of the above observations also apply to chainlike crowders. In Fig. 3 *b*, we consider chainlike polymeric crowders of different sizes. The results show that as the increase of chain length m_C is essentially equivalent to an increase in crowder size σ_C in Fig. 3 *a*, crowding enhances folding at low c_C but stabilizes the denatured ubiquitin at high c_C.

In the previous two figures, the size of the native ubiquitin was fixed at $\sigma_P = 2.4\,\text{nm}$. Because the size of the native protein affects the volume accessible to the crowders as folding occurs, one would expect the variation in σ_P to affect the influence of the crowders. For example, smaller σ_Ps would be expected to broaden the range over which folding is enhanced, with larger σ_Ps having an opposite effect, for reasons already described above. The results shown in Fig. 3 *c*, where the effect of the size of the native ubiquitin is examined (with the crowder assumed to be spherical with a size of $\sigma_C = 0.5\,\text{nm}$), confirm the expectations. The results, as also emphasized by Zhou and Hall (16) for the pure HS interactions, imply that the crowding effect is quite sensitive to the size of the native protein and that sufficiently accurate size estimation is necessary to predict the extent of enhancement or decrease in the equilibrium.

In summary, we note that in general smaller crowders serve as denaturants and stabilize the nonnative form, whereas the larger crowders (at low enough concentrations) promote the stability of the folded form. These predictions are consistent with Timasheff's hypothesis (31) based on experimental observations that denaturants tend to preferentially bind to the proteins and prevent folding and that stabilizers are preferentially excluded from the protein domains, thereby allowing folding, as also observed by Zhou and Hall (16). Deviations from this rule may occur and could arise from interactions other than pure excluded-volume interactions. This is alluded to by our results for the cases of nonbonded attractive interactions, which shift the quantitative predictions substantially under certain conditions. See, for example, the results in Fig. 3 *a* for the HSC model and one with the SW nonbonded interactions for $\sigma_C = 0.5\,\text{nm}$ around a crowder concentration of 5 mol/L; whereas the pure HSC approximation predicts enhancement of folding by $\sim$15% from the initial equilibrium, the model with nonbonded interactions actually shows a 40% downward shift toward denaturation.

Coagulation (or coalescence)

The second reaction we consider is coagulation of three reactant molecules into a product molecule,

$$3R \rightleftharpoons P, \tag{16}$$

where the reactant R and product P are modeled, respectively, as small and large single spherical particles ($m_R = m_P = 1$). Note that if one takes the volume of one P molecule to be identical to that of the three R molecules of size $\sigma_R = 1\,\text{nm}$, the size of P will be approximately $\sigma_P = 1.44\,\text{nm}$ (corresponding to the coalescence of liquid drops). We consider the effect of chainlike crowders (Fig. 4) as well as those of variations in the size of the crowder segment (Fig. 5 *a*) and product molecule (Fig. 5 *b*).

It is more instructive to begin with the case of increase in the chain length of the crowder first (Fig. 4). For this, we fix the segment size at $\sigma_C = 0.2\,\text{nm}$ (well below the size of the reactant, σ_R, taken to be 1 nm). The product size is fixed at $\sigma_P = 1.55$ nm, slightly above the magnitude expected for coalescence (volume conservation). The line corresponding to monomers ($m_C = 1$) in Fig. 4 *a* shows that the reactant dispersion remains stable, with a gradual reduction in α as the molar concentration of the crowder increases. The reduction in α arises from the fact that (analogous to the case discussed in Fig. 3 *a* above) the formation of the product (which would cause a larger excluded volume for the crowder) affects the configurational entropy of the crowder. Further, the smaller crowder molecules can take up the space between the reactants and prevent mutual contacts between the reactant molecules. The large size difference between the reactant and the crowder could lead to depletion attraction between the reactants (known as the Asakura-Oosawa interaction) (32), thus promoting coagulation, at large crowder concentrations (see Hiemenz and Rajagopalan (33)), but this effect is not seen here because we have not accounted for depletion attraction caused by the crowders. In contrast, for polymeric crowders, that is, as for chain length m_C of the order of 10 or larger, coagulation is enhanced (i.e., α increases) at small values of the crowder concentration because the formation of the coagulated product decreases the excluded volume for the crowders. However, as the crowder concentration increases further, the degree of reaction reaches a maximum and begins to decrease as shifting the equilibrium toward the (smaller) reactant molecules provides a greater degree of freedom for the crowder chains. Here, again, the behavior is analogous to what is seen in Fig. 3 *b* for the folding transition. Similar results are seen for further increases in m_C, with larger and sharper changes in α with crowder concentration. In all cases, the inclusion of nonbonded SW interactions enhances the reaction less at lower crowder concentrations but retards the reaction less at higher concentrations for the same reasons discussed in the similar context for the folding transition.

It is instructive to examine the above results in terms of the volume fraction of the crowder instead of the molar fraction. This is illustrated for the coagulation reaction in Fig. 4 *b*. Fig. 4 *b*, which describes the case discussed above (the effect of chain length), shows that the decrease in α is quite sharp in terms of volume fraction for monomeric crowders. For polymeric crowders, the bell-shaped curves seen in Fig. 4 *a* for $m_C = 100$ can be seen for all values of m_C clearly. Moreover, coagulation is completely arrested for a volume fraction of ~0.25, and the behavior for $m_C > \sim 50$ becomes very close to each other, indicating that for large chains, the volume fraction of the crowder is the dominant determinant for the degree of reaction. The maximum α occurs around a volume fraction of ~0.16 regardless of the chain length (for $m_C > 50$), and this value could be used to determine the molar fraction needed for optimum enhancement of the reaction.

In view of the discussion above, the results illustrated in Fig. 5 *a* for the effect of segment size in a chainlike crowder of $m_C = 100$ are straightforward to interpret. Again, the results show that the qualitative behavior (as a function of crowder concentration and segment size) is dictated by the

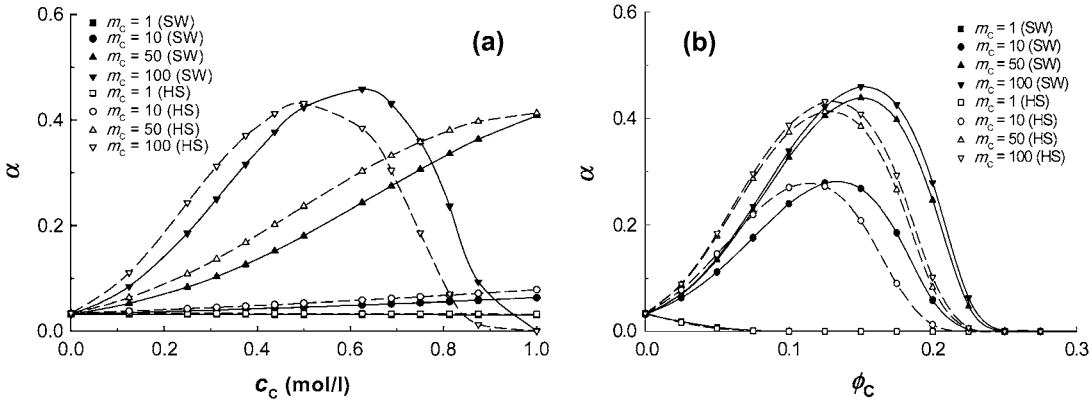

FIGURE 4 Degree of reaction α for coagulation $3R \rightleftharpoons P$ as a function of (*a*) molar concentration and (*b*) volume fraction of crowder C for the effect of the chain length of the crowder. Solid lines correspond to situations in which nonbonded SW interactions are included, whereas the dashed lines correspond to only the HS interactions. It has been assumed that $c_R^0 = 0.1\,\text{mol/l}$, $m_R = 1$, $\sigma_R = 1\,\text{nm}$, $m_P = 1$, $\sigma_P = 1.55\,\text{nm}$, and $\sigma_C = 0.20\,\text{nm}$.

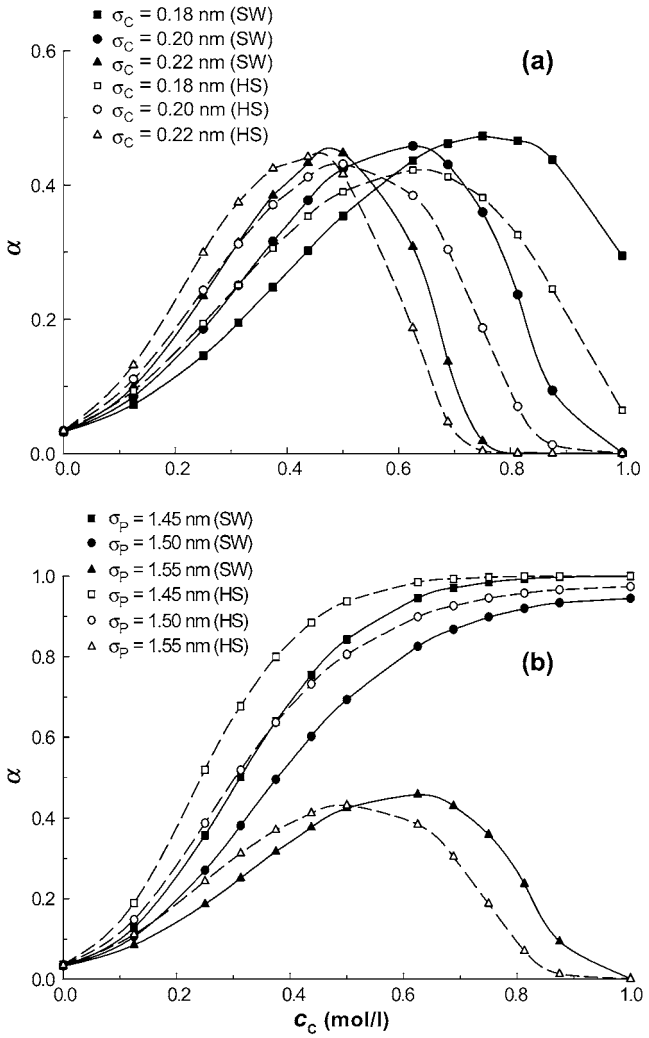

FIGURE 5 Degree of reaction α for coagulation $3R \rightleftharpoons P$ as a function of the molar concentration of crowder C. Solid lines correspond to situations in which nonbonded SW interactions are included, whereas the dashed lines correspond to only the HS interactions. For both cases shown below, it has been assumed that $c_R^0 = 0.1\,\text{mol/l}$, $m_R = 1$, $\sigma_R = 1\,\text{nm}$, $m_P = 1$, and $m_C = 100$. (*a*) The effect of the size of crowder; $\sigma_P = 1.55\,\text{nm}$. (*b*) The effect of the size of product; $\sigma_C = 0.20\,\text{nm}$.

sizes of the molecules, although quantitative adjustments resulting from other interactions could be substantial, as evident from the effect of the SW interactions.

The effect of the product size σ_P as shown in Fig. 5 *b* is also instructive. As σ_P decreases from $\sigma_P = 1.55\,\text{nm}$, α increases, as expected, because the volume excluded by the product decreases, and the reaction moves toward coagulation. At $\sigma_P = 1.45\,\text{nm}$ (corresponding roughly to volume conservation between the reactant and product), α monotonically increases with crowder concentration c_C (because the product formation enhances the configurational entropy of the crowder chains). As suggested by Minton, the crowding effect in this case (and for smaller product sizes) would be to enhance the reaction.

Results such as those above can be used to develop scaling relations for α in terms of the crowder type, size, and chain length. We have not attempted to do so here because the resulting scaling relations will not be of much value unless all the necessary molecular interactions are incorporated in the model.

Polymerization (or association)

Finally we consider a polymerization reaction with n reactant molecules R forming a chain molecule P_3. We take n to be 3 to examine the consequences and, at the same time, to investigate the effect of the shape of the product molecule (i.e., the difference between assuming the product to be a single spherical molecule and assuming it to be chainlike):

$$3R \rightleftharpoons P_3, \tag{17}$$

where the product P_3 is a linear chain molecule of three connected identical spherical segments. Initially the segment size P_3 is taken to be the same as the size of the reactant molecule R ($\sigma_R = \sigma_P = 1.0\,\text{nm}$; Figs. 6 and 7 *a*), but subsequently small variations in σ_P are explored (Fig. 7 *b*).

The general qualitative arguments already presented for the earlier cases apply as well for all the results here. For example, Fig. 6 *a*, which illustrates the effect of the length m_C of the crowder, shows that an enhancement in the reaction occurs as the chain length of the crowder is increased for the same molar concentration. It is also clear that a short crowder ($m_C = 1$ or 10) only marginally enhances the extent of reaction, whereas longer chains significantly alter the reaction degree, consistent with experimental observation (34). Again this observation holds for a fixed molar concentration, not for the same volume fraction of the crowder, as we discuss later. Further, it may not be clear from Fig. 6 *a* that even for monomeric crowders an enhancement is seen in this case; we illustrate this later when we discuss the results in terms of the volume fraction of the crowders.

Fig. 7 *a*, presented for $m_C = 100$ so that the differences illustrated can be seen clearly, shows that small variations in the segment size of the crowder could lead to noticeable changes in α, with larger segment sizes shifting the reaction equilibrium toward the product. A more pronounced sensitivity is seen in Fig. 7 *b* for small variations in the segment size of the product P (with σ_R still fixed at 1 nm, and again for $m_C = 100$), with smaller σ_Ps favoring the formation of the product. It appears that the above sensitivity arises from what drives the reaction forward. Considering, for example, $\sigma_R = \sigma_P = 1\,\text{nm}$ and monomeric crowder, one notes that there is small saving in excluded volume (for the crowder) when three R molecules form a three-segment chain of P_3. It is this increase in volume available for the crowder that drives the reaction forward. The extent of enhancement understandably increases for longer crowders at any given molar concentration of crowder. The above reduction in excluded volume for the crowder increases further for smaller σ_Ps, thereby pushing the reaction forward more even for monomeric crowders.

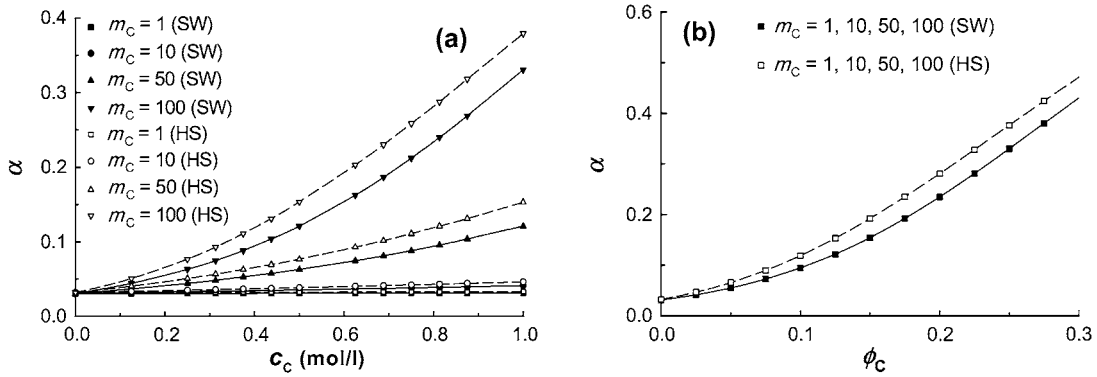

FIGURE 6 Degree of reaction α for polymerization $3R \rightleftharpoons P_3$ as a function of (*a*) molar concentration and (*b*) volume fraction of crowder *C* for the effect of the chain length of the crowder. Solid lines correspond to situations in which nonbonded SW interactions are included, whereas the dashed lines correspond to only the HS interactions. It has been assumed that $c_R^0 = 0.1$ mol/l, $m_R = 1$, $\sigma_R = 1$ nm, $m_P = 3$, $\sigma_P = 1$ nm, and $\sigma_C = 0.20$ nm.

As noted earlier, the fact that the reaction is enhanced even for monomeric crowders may not be evident from Fig. 6 *a*, but the increase in α can be seen from Fig. 6*b*, which shows the results in Fig. 6 *a* instead in terms of volume fraction. Interestingly, for the parameters shown, the numerical results for α in Fig. 6 *b* for all values of m_C are indistinguishable from each other, for both the HSC model as well as the one with nonbonded SW attraction, indicating that the increase in α is essentially the same regardless of the length of the crowder as long as the volume fraction (or mass fraction) of the crowder is the same. That is, somewhat counterintuitively, the results show that it makes no difference whether the crowders are present as monomers or as a polymeric chain, despite the potential entropic gain in monomeric form. This result simply indicates that the shift in the reaction is driven by the free energy changes arising from the reactant and the product rather than a significant contribution from the crowders. However, the difference exists between monomeric and polymeric crowders for other cases, e.g., when σ_R and σ_P are different. For instance, at $\sigma_R = 1$ nm and $\sigma_P = 0.99$ nm, the increase in available volume in this case does make a difference for monomeric crowders, but the advantage quickly vanishes for longer crowders, for reasons mentioned above. Similar results are obtained for other values of σ_P.

We note that a comparison of Figs. 4 and 5 with Figs. 6 and 7 reveals the sharp differences between the cases of a compact, spherical shape of the product and a chainlike product. Particularly relevant in this context are Fig. 4 and Fig. 6, which use the same parameters for the reactant and the crowder but differ only in the shape of the product; i.e., in the case of Fig. 4, the product is assumed to be a sphere of roughly the same volume as that of the three reactant molecules, whereas in Fig. 6, the product is a chainlike assembly of the three reactant molecules. The comparison shows that although the relative influences caused by variations in the size of the crowder segment (Figs. 5 *a* and 7 *a*) and by the chain length of the crowder (Figs. 4 and 6) remain the same, there are drastic differences in the extent of influence of the crowder concentration. In particular, the enhancement in the reaction is sharper in the case of a spherical product with the addition of the crowder. For example, referring to Figs. 5 *a* and 7 *a*, one sees that, for $\sigma_C = 0.2$ nm, at a crowder concentration of 0.4 mol/L, the enhancement in the reaction is ~4 times larger in the case of a spherical product than for a chainlike product (α is ~0.36 in the case of spherical product, as opposed to an α of ~0.09 for chainlike product; the initial α is ~0.03 in both cases).

Finally, it is also worth noting that although the results here for polymerization/self-association show a monotonic increase in α (except when the segment size of the associated chain makes it unfavorable), a more complex behavior could be expected for products of much larger chain lengths because the configurational entropy and possibilities of preferential binding or exclusion of the crowders change with increasing chain length of the product.

CONCLUDING REMARKS

The molecular thermodynamic model presented avoids the need for extensive computer simulations but can provide guidance for the selection of crowders for enhancing or retarding conformational isomerization of proteins, coagulation or molten, amorphous polymerization, or self-association. Although simple hard-core excluded-volume arguments (which have been used extensively in various forms) can in general predict the qualitative aspects of the effects of crowders, the results show that other intermolecular interactions can substantially alter the extent of enhancement or reduction of the equilibrium and could even change the direction of the shift. The results show that a coarse-grained approach can offer sufficient guidance in many cases, if not all, but the capability of the model to explain and predict the reaction equilibria depends on whether the inter- and intramolecular interactions and molecular structures are taken into account in a reasonable manner. From this point of view, more exact potential

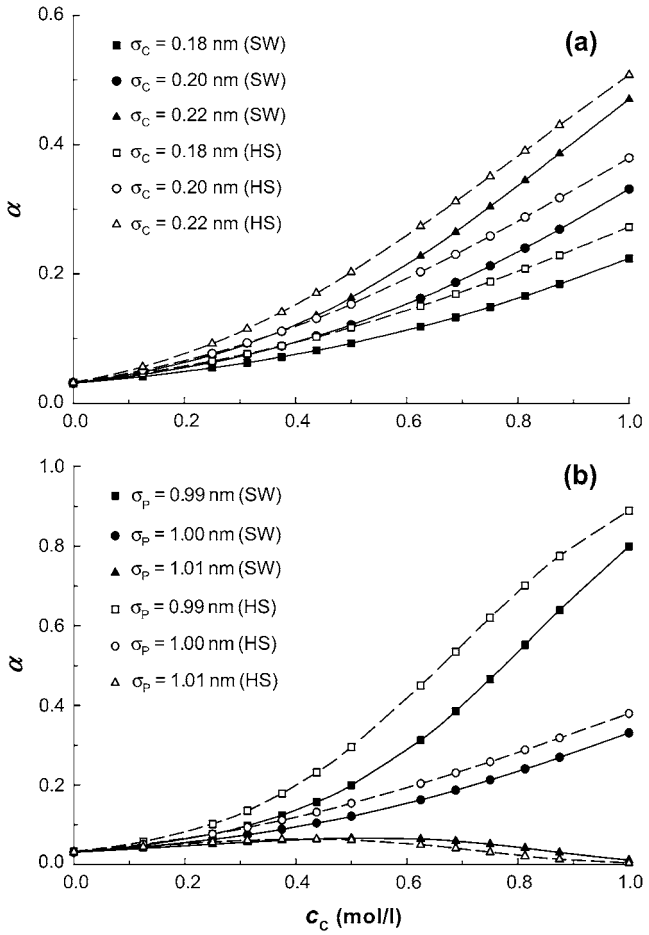

FIGURE 7 Degree of reaction α for polymerization $3R \rightleftharpoons P_3$ as a function of the molar concentration of crowder C. Solid lines correspond to situations in which nonbonded SW interactions are included, whereas the dashed lines correspond to only the HS interactions. For both cases shown below, it has been assumed that $c_R^0 = 0.1\,\text{mol/l}$, $m_R = 1$, $\sigma_R = 1\,\text{nm}$, $m_P = 3$, and $m_C = 100$. (*a*) The effect of the size of crowder; $\sigma_P = 1\,\text{nm}$. (*b*) The effect of the size of product; $\sigma_C = 0.20\,\text{nm}$.

models and more realistic conformational details for the reactant, product, and crowder can be included to construct theoretical models capable of precisely describing the crowding effects. In particular, our results show that short-range interactions are important for accurately describing the effects of crowders. More realistically, electrostatic, hydrophobic, associating, solvent-induced, and other interactions, may be incorporated to elucidate the crowding effects quantitatively (35,36).

As emphasized by Minton (4), although there are many experimental reports on the effects of crowders on folding and refolding reactions, many of the proteins studied or of interest exist as homo-oligomers, and the interpretation for the thermodynamics and kinetics of their conformational behavior is complicated by the coupling of folding and association. An advantage of the approach presented here is that competing reactions can be incorporated within the model.

Support from the National University of Singapore is gratefully acknowledged.

REFERENCES

1. Minton, A. P. 2001. The influence of macromolecular crowding and macromolecular confinement on biochemical reactions in physiological media. *J. Biol. Chem.* 276:10577–10580.
2. Ellis, R. J., and A. P. Minton. 2003. Cell biology—Join the crowd. *Nature*. 425:27–28.
3. Sasahara, K., P. McPhie, and A. P. Minton. 2003. Effect of dextran on protein stability and conformation attributed to macromolecular crowding. *J. Mol. Biol.* 326:1227–1237.
4. Minton, A. P. 2005. Influence of macromolecular crowding upon the stability and state of association of proteins: predictions and observations. *J. Pharm. Sci.* 94:1668–1675.
5. Hall, D., and A. P. Minton. 2003. Macromolecular crowding: qualitative and semiquantitative successes, quantitative challenges. *Biochim. Biophys. Acta. Proteins Proteom.* 1649:127–139.
6. Wilf, J., and A. P. Minton. 1981. Evidence for protein self-association induced by excluded volume myoglobin in the presence of globular-proteins. *Biochim. Biophys. Acta*. 670:316–322.
7. Minton, A. P. 2000. Implications of macromolecular crowding for protein assembly. *Curr. Opin. Struct. Biol.* 10:34–39.
8. Schnell, S., and T. E. Turner. 2004. Reaction kinetics in intracellular environments with macromolecular crowding: simulations and rate laws. *Prog. Biophys. Mol. Biol.* 85:235–260.
9. Aranda, J. S., E. Salgado, and A. Munoz-Diosdado. 2006. Multifractality in intracellular enzymatic reactions. *J. Theor. Biol.* 240:209–217.
10. Zorrilla, S., M. Jimenez, P. Lillo, G. N. Rivas, and A. R. Minton. 2004. Sedimentation equilibrium in a solution containing an arbitrary number of solute species at arbitrary concentrations: theory and application to concentrated solutions of ribonuclease. *Biophys. Chem.* 108:89–100.
11. Minton, A. P. 1981. Excluded volume as a determinant of macromolecular structure and reactivity. *Biopolymers*. 20:2093–2120.
12. Minton, A. P., and H. Edelhoch. 1982. Light-scattering of bovine serum-albumin solutions—extension of the hard particle model to allow for electrostatic repulsion. *Biopolymers*. 21:451–458.
13. Minton, A. P. 1995. A molecular-model for the dependence of the osmotic-pressure of bovine serum-albumin upon concentration and pH. *Biophys. Chem.* 57:65–70.
14. Minton, A. P. 2000. Effect of a concentrated ''inert'' macromolecular cosolute on the stability of a globular protein with respect to denaturation by heat and by chaotropes: a statistical-thermodynamical model. *Biophys. J.* 78:101–109.
15. Berg, O. G. 1990. The influence of macromolecular crowding on thermodynamic activity—solubility and dimerization constants for spherical and dumbbell-shaped molecules in a hard-sphere mixture. *Biopolymers*. 30:1027–1037.
16. Zhou, Y. Q., and C. K. Hall. 1996. Solute excluded-volume effects on the stability of globular proteins: a statistical thermodynamic theory. *Biopolymers*. 38:273–284.
17. Kinjo, A. R., and S. Takada. 2002. Effects of macromolecular crowding on protein folding and aggregation studied by density functional theory: dynamics. *Phys. Rev. E.* 66:051902.
18. Kinjo, A. R., and S. Takada. 2002. Effects of macromolecular crowding on protein folding and aggregation studied by density functional theory: statics. *Phys. Rev. E.* 66:031911.
19. Dima, R. I., and D. Thirumalai. 2002. Exploring protein aggregation and self-propagation using lattice models: phase diagram and kinetics. *Protein Sci.* 11:1036–1049.
20. Smith, A. V., and C. K. Hall. 2001. Protein refolding versus aggregation: computer simulations on an intermediate-resolution protein model. *J. Mol. Biol.* 312:187–202.

21. Harrison, P. M., H. S. Chan, S. B. Prusiner, and F. E. Cohen. 1999. Thermodynamics of model prions and its implications for the problem of prion protein folding. *J. Mol. Biol.* 286:593–606.

22. Elcock, A. H. 2003. Atomic-level observation of macromolecular crowding effects: escape of a protein from the GroEL cage. *Proc. Natl. Acad. Sci. USA.* 100:2340–2344.

23. Mansoori, G. A., N. F. Carnahan, K. E. Starling, and T. W. Leland. 1971. Equilibrium thermodynamic properties of the mixture of hard spheres. *J. Chem. Phys.* 54:1523–1525.

24. Barker, J. A., and D. Henderson. 1967. Perturbation theory and equation of state for fluids—square-well potential. *J. Chem. Phys.* 47:2856–2861.

25. Gil-Villegas, A., A. Galindo, P. J. Whitehead, S. J. Mills, G. Jackson, and A. N. Burgess. 1997. Statistical associating fluid theory for chain molecules with attractive potentials of variable range. *J. Chem. Phys.* 106:4168–4186.

26. Chapman, W. G., K. E. Gubbins, G. Jackson, and M. Radosz. 1990. New reference equation of state for associating liquids. *Ind. Eng. Chem. Res.* 29:1709–1721.

27. Jiang, J. W., and J. M. Prausnitz. 1999. Equation of state for thermodynamic properties of chain fluids near-to and far-from the vapor-liquid critical region. *J. Chem. Phys.* 111:5964–5974.

28. Karasawa, T., K. Tabuchi, M. Fumoto, and T. Yasukawa. 1993. Development of simulation-models for protein-folding in a thermal annealing process.1. A simulation of BPTI folding by the pearl necklace model. *Comput. Appl. Biosci.* 9:243–251.

29. Fox, T., and P. A. Kollman. 1996. The application of different solvation and electrostatic models in molecular dynamics simulations of ubiquitin: how well is the x-ray structure ''maintained''? *Proteins.* 25:315–334.

30. Scharnagl, C., M. Reif, and J. Friedrich. 2005. Stability of proteins: temperature, pressure and the role of the solvent. *Biochim. Biophys. Acta.* 1749:187–213.

31. Timasheff, S. N. 1993. The control of protein stability and association by weak-interactions with water—how do solvents affect these processes. *Annu. Rev. Biophys. Biomol. Struct.* 22:67–97.

32. Asakura, S., and F. Oosawa. 1958. Interaction between particles suspended in solutions of macromolecules. *J. Polym. Sci.* 33:183–192.

33. Hiemenz, P. C., and R. Rajagopalan. 1997. Principles of Colloid and Surface Chemistry, 3rd ed. Taylor & Francis, New York.

34. Winzor, D. J., and P. R. Wills. 2006. Molecular crowding effects of linear polymers in protein solutions. *Biophys. Chem.* 119:186–195.

35. Minton, A. P. 2006. How can biochemical reactions within cells differ from those in test tubes? *J. Cell Sci.* 119:2863–2869.

36. Du, F., Z. Zhou, Z. Y. Mo, J. Z. Shi, J. Chen, and Y. Liang. 2006. Mixed macromolecular crowding accelerates the refolding of rabbit muscle creatine kinase: implications for protein folding in physiological environments. *J. Mol. Biol.* 364:469–482.